

Ion Heating Due to Double-Layer Disruption in a Plasma

K. Saeki, S. Iizuka, and N. Sato

Department of Electronic Engineering, Tohoku University, Sendai 980, Japan

(Received 3 June 1980)

A new mechanism is presented for ion heating in a plasma penetrated by an electron beam. Oscillating potentials comparable to the electron-beam energy are observed below the threshold of the stable double-layer formation. These fluctuations (formation and disruption of double layers) accelerate, trap, and detrap thermal ions, resulting in highly energetic ion bursts, which form a tail on the ion-energy distribution function.

PACS numbers: 52.50.Gj, 52.35.Fp

Recently, the nonlinear evolution of the electron-ion two-stream instability (the Buneman instability)¹ into double layers² in plasmas has attracted intense attention. Double layers have been observed³ near onset of this instability. Iizuka *et al.*⁴ revealed clearly that the Pierce instability⁵ following the Buneman instability results in the formation of double layers in a bounded plasma. On the other hand, the Buneman instability has been regarded as one of the effective heating mechanisms in current-carrying plasmas.⁶ Anomalous resistivity and electron heating due to the Buneman instability have been discussed based on the quasilinear theory.⁷ A theory taking the formation of several double layers into account has also been presented.⁸ This Letter reports ion heating due to double-layer disruption in an electron-beam-plasma system. Below the threshold of the stable double-layer formation, there appear large-amplitude fluctuations $e\bar{\phi} \approx eV_b \gg T_e$, which are interpreted as successive formations and disruptions ($\bar{\phi}$, potential fluctuation; V_b , acceleration voltage of the electron beam; T_e , electron temperature). These fluctuations produce intense ion bursts (ballistic ions)⁹ which form a tail on the ion-energy distribution function.

The apparatus used in these experiments is illustrated in Fig. 1(a). The experimental region [between a mesh anode *A* (at an axial location $z = 0$) and a 6-cm-diam plasma emitter PE (at $z = L = 10$ cm)] is filled with a potassium plasma of density $n = 10^6 - 10^7$ cm⁻³ and temperature $T_e \approx T_i \approx 0.2$ eV, supplied by the plasma emitter.^{4,10} Both the mesh anode and the plasma emitter are grounded. An electron beam is injected into this region from a 6-cm-diam oxide cathode biased at a beam voltage V_b (1–10 V). A control voltage V_c applied to a control grid G_c is able to increase the beam density linearly, if V_b is constant and the cathode is heated enough. The plasma is collisionless because background pressure $\approx 5 \times 10^{-6}$ Torr. The plasma parameters are measured by

a Langmuir probe, an emissive probe, and an ion-energy analyzer.

Figure 1(b) shows the dependence of the electron current I_p (picked up by the Langmuir probe at $z = 7$ cm) and the space potential ϕ (the floating potential of the emissive probe at $z = 2$ cm) on the sawtooth voltage V_c . Although the beam current captured by the mesh anode increases linearly with an increase in V_c , I_p and ϕ behave in complicated manners, as shown by control-voltage regimes (A)–(D). No instability is observed in regime (A). The space potential ϕ is uniform along z and almost equal to the ground potential. The beam current is proportional to V_c . In regime (B), the average beam current still increases linearly with V_c . The space potential

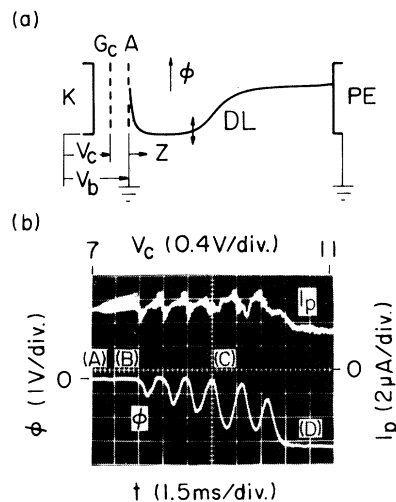


FIG. 1. (a) Experimental apparatus. The beam density is varied by control grid G_c . *K*, oxide cathode; *A*, mesh anode (at an axial position $z = 0$); *PE*, plasma emitter (at $z = L = 10$ cm). (b) The stability of electron-beam-plasma system. $V_b = 3$ V; $n = 3 \times 10^6$ cm⁻³. Regime (A), stable and homogeneous state; regime (B), the Buneman instability; regime (C), repetition of double-layer formation and disruption; regime (D), stable double layer.

fluctuates at a low level in amplitude $e\bar{\phi}/T_e \approx 1$, although the dc potential is still nearly equal to the ground potential. This instability has an average frequency of 80 kHz [$\approx 0.3(\omega_{pb}\omega_{pi}^2)^{1/3}/2\pi$ at $k_D L/\pi = 1.8$], being identified as the Buneman instability.⁴ Here, ω_{pb} , ω_{pi} , and k_D are the plasma frequencies of beam electrons and plasma ions, and the Debye wave number of plasma electrons, respectively. Still higher voltage V_c [i.e., higher beam current, regime (D)] leads to the nonoscillatory Pierce instability,⁵ limiting the beam current. A large negative dc potential well in front of the anode, generated by the Pierce instability, results in the formation of a stable double layer in the region between the anode and the plasma emitter.⁴ In control-voltage regime (C), large potential fluctuations are observed. The beam current of this region is close to that calculated from a critical ω_{pb} determined by $(\omega_{pb}/U)^2 \sim (\pi/L)^2 + k_D^2$ ($eV_b = m_e U^2/2$).⁴ The maximum peak-to-peak amplitude $\bar{\phi}$ is found to be $\approx V_b$ ($\gg T_e/e$). Thus, these fluctuations are expected to have large effects on the ion motion.

To investigate the behavior of plasma ions in

these four characteristic regimes, the ion-energy analyzer facing the electron-beam source is set at $z = 8$ cm where the space potential is perturbed at a low level. The dependence of the ion-collector current on the collector voltage is shown in Fig. 2(a). When $V_c < 4$ V and $V_c > 15$ V, the normal Maxwellian distribution of ion energy is obtained with $T_i \approx 0.2$ eV, equal to the temperature of ions emitted from the plasma emitter. For $4 \text{ V} < V_c < 15 \text{ V}$, however, a high-energy tail is observed on the ion-energy distribution function. At $V_c = 8$ V, the temperature of the bulk ions is 0.3 eV, and that of the high-energy tail T_{it} is 1.1 eV, several times larger than that of the initial plasma. The relation between $\bar{\phi}$ and T_{it} may be understood by comparing Figs. 2(b) and 2(c). In the regime of the Buneman instability (B), high-frequency (~ 80 kHz) and small-amplitude ($e\bar{\phi} \approx T_e$) oscillations are observed in the whole experimental region. In the regime (C), however, low-frequency (2–10 kHz) and large-amplitude ($e\bar{\phi} \approx eV_b$) oscillations are detected in the region from $z = 0$ to 4.5 cm which corresponds to the potential well in case of the

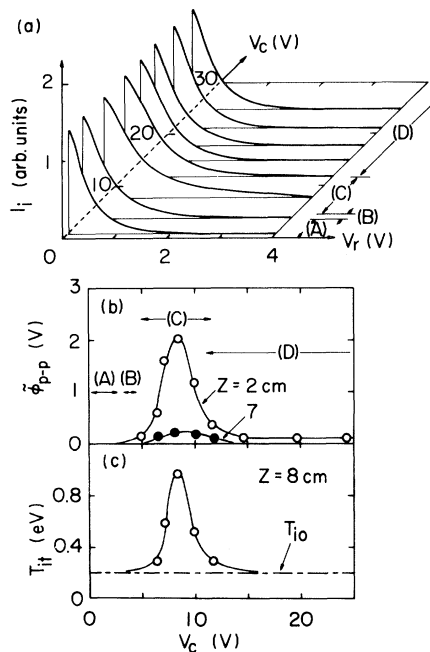


FIG. 2. (a) The dependence of ion-collector current I_i on retarding voltage V_r with control voltage V_c as a parameter. $V_b = 3$ V; $z = 8$ cm. (b) Peak-to-peak potential fluctuations $\bar{\phi}_{p-p}$ and (c) temperature of high-energy tail T_{it} vs V_c . T_{i0} is the temperature of ions emitted from PE.

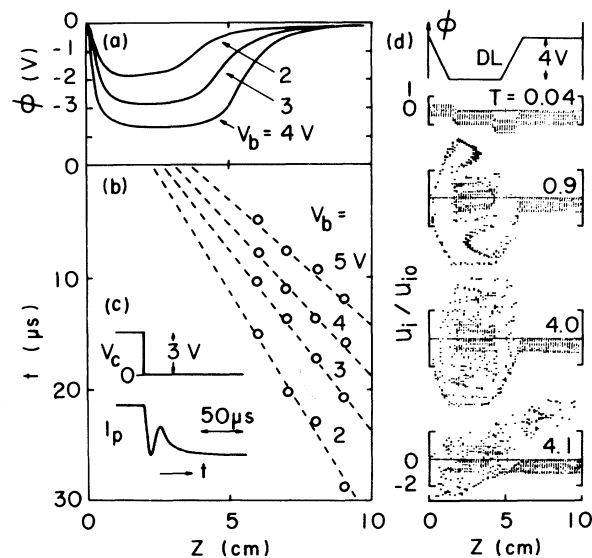


FIG. 3. Simulation of ion-burst formation. (a) Potential profiles of double layers. (b) Propagation and (c) temporal form (at $z = 8$ cm) of ion bursts after turning off the double layers. (d) Computer simulation of trapping and detraping due to double-layer formation and disruption. u_i/u_{i0} is the ion velocity normalized by the ion thermal velocity u_{i0} of the initial plasma. Double layer is turned on at a normalized time $T = tu_{i0}/L = 0$, and is turned off at $T = 4.0$. Here, L is the length of the experimental region.

stable double layers (D). At $z = 7$ cm, the fluctuation ϕ is $\approx T_e/e$. The behavior of the beam current suggests that the fluctuations are relaxation oscillations between regimes (B) and (D), as explained qualitatively as follows. The double-layer formation decreases the beam current below the threshold of the Pierce instability, because of its large potential well. The resultant beam current does not sustain the well, and the potential returns to the initial homogeneous one, which allows again the initial beam current, enough to excite the Pierce instability.

In order to clarify the ion-heating mechanism, we turn on and off the double layers by pulsing the bias V_c . The ion collector current of the analyzer (biased at 1 V) at $z = 8$ cm shows intense ion bursts only when the double layers are turned off. The movable Langmuir probe is used to investigate the behavior of the bursts temporally and spatially, because the heat from the cathode and the plasma emitter decreases the quality of the analyzer when it approaches them. The ion bursts are shielded by the plasma electrons. Consequently, the plasma-electron current to the probe contains direct information on the density of the ion bursts. Figures 3(c) and 3(b) show observed signals and space-time plots of the ion bursts, respectively, after turning off the electron beam at a time $t = 0$. The time delay of the signals indicates that the average energy of the bursts is about 60% of the electron-beam energy eV_b . The profiles of the stationary double layers for each V_b are shown in Fig. 3(a). The depth of the potential well is nearly equal to V_b . From Figs. 3(a) and 3(b), the origin of the bursts is concluded to be at the bottom of the potential well.

The simple computer simulation concerning the phase-space orbits of ions in the potential ϕ varying similarly to the repetition of the double-layer formation and disruption is shown in Fig. 3(d). The sudden drop of the potential is observed to form the trapped ions, which consist of two groups. One of them is the group which was around $z = 2.5$ cm and the other is the group which was on the slope of the potential ϕ when ϕ started to drop. The latter group is accelerated and trapped in the potential well, having a high kinetic energy. This forms intense ion bursts (de-

trapping)¹¹ in both directions after ϕ returns to the initial homogeneous state. The temporal form of the ion bursts in Fig. 3(c) agrees well with the time-dependent number of ions found at $z = 8$ cm in Fig. 3(d). A simulation is also carried out for sinusoidal oscillations of the potential ϕ , as shown in Fig. 1(b). The resultant trapped ions have a broad energy distribution function, which provides the formation of the high-energy tail in Fig. 2(a) after their detrapping.

We thank Professor Y. Hatta for his encouragement. We also thank Dr. J. Juul Rasmussen for his critical reading of the manuscript. We are indebted to H. Ishida for his assistance in constructing the apparatus.

¹O. Buneman, Phys. Rev. Lett. **1**, 8 (1958), and Phys. Rev. **115**, 503 (1959).

²L. P. Block, Cosmic Electroduct. **3**, 349 (1972); S. Torvén and D. Andersson, J. Phys. D **12**, 717 (1979); P. Coakley and N. Hershkowitz, Phys. Fluids **22**, 1171 (1979); J. S. Levine, F. W. Crawford, and D. B. Ilić, Phys. Lett. **65A**, 27 (1978); T. Sato and H. Okuda, Phys. Rev. Lett. **44**, 740 (1980).

³E. I. Lutsenko, N. D. Seveda, and L. M. Konstsevoi, Zh. Eksp. Teor. Fiz. **69**, 2067 (1975) [Sov. Phys. JETP **42**, 1050 (1976)]; B. H. Quon and A. Y. Wong, Phys. Rev. Lett. **37**, 1393 (1976).

⁴S. Iizuka, K. Saeki, N. Sato, and Y. Hatta, Phys. Rev. Lett. **43**, 1404 (1979).

⁵J. R. Pierce, J. Appl. Phys. **15**, 721 (1944).

⁶S. M. Hamberger and J. Jancarik, Phys. Rev. Lett. **25**, 999 (1970).

⁷R. C. Davidson, N. A. Krall, K. Papadopoulos, and R. Shanny, Phys. Rev. Lett. **24**, 579 (1970); T. D. Mantei and D. Gresillon, Phys. Rev. Lett. **40**, 1383 (1978).

⁸J. S. DeGroot, C. Barnes, A. E. Walstead, and O. Buneman, Phys. Rev. Lett. **38**, 1283 (1977).

⁹I. Alexeff, W. D. Jones, and K. Lonngren, Phys. Rev. Lett. **21**, 878 (1968); H. Ikezi and R. J. Taylor, J. Appl. Phys. **41**, 738 (1970).

¹⁰K. Saeki, S. Iizuka, N. Sato, and Y. Hatta, Appl. Phys. Lett. **37**, 37 (1980).

¹¹For example, T. P. Starke and J. M. Malmberg, Phys. Rev. Lett. **37**, 505 (1976); N. Sato, G. Popa, E. Märk, R. Schrittwieser, and E. Mravlag, Phys. Rev. Lett. **37**, 1684 (1976); N. Sato, K. Saeki, and R. Hatakeyama, Phys. Rev. Lett. **38**, 1480 (1977).

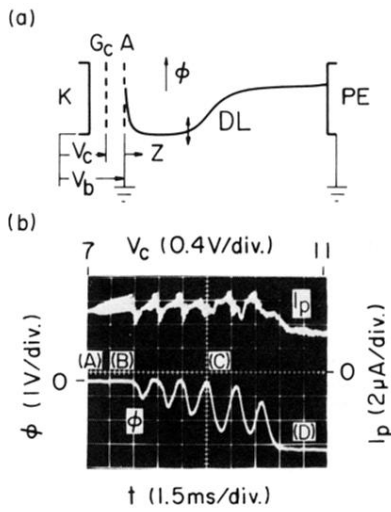


FIG. 1. (a) Experimental apparatus. The beam density is varied by control grid G_c . K , oxide cathode; A , mesh anode (at an axial position $z=0$); PE , plasma emitter (at $z=L=10$ cm). (b) The stability of electron-beam-plasma system. $V_b=3$ V; $n=3\times 10^6$ cm $^{-3}$. Regime (A), stable and homogeneous state; regime (B), the Buneman instability; regime (C), repetition of double-layer formation and disruption; regime (D), stable double layer.